

Authors' response to comments:

We would like to thank the two reviewers and the associate editor, Marcel van der Meer, for their positive and constructive comments on our manuscript. In the new version of the manuscript, we have expanded the description and discussion of the NMR experiments and have refined our presentation of the compound specific isotope data. Below, we detail our response to both reviewers' comments and have inserted a revised version of the manuscript with tracked changes.

Response to Reviewer 1

In this article, the authors report on the structural identification of a recently discovered class of archaeal membrane lipids, the butanetriol and pentanetriol dialkyl glycerol tetraethers (BDGTs and PDGTs) using 1D and 2D NMR techniques on isolated BDGT-0. In addition, their occurrence and possible source organisms in contrasting environmental settings is discussed, notably in the light of the stable carbon isotopic composition of the biphytane alkyl chain (bp-0) released upon ether cleavage compared to that of bp-0 from GDGTs, methane, TOC and DIC from the corresponding sediment samples. Overall, this manuscript is very well written, easy and pleasant to read, the data seem reliable and the interpretations are generally well argued and convincing. I have, however, a few (minor) points to be discussed and commented prior acceptance for publication in Biogeosciences.

The first point deals with the NMR structural characterization of BDGT-0. The authors conducted top-quality work to isolate ca. 0.9 mg of BDGT-0 with a high purity, and use high tech NMR material to perform the 1D and 2D experiments necessary for full characterization. However, in the manuscript, the description of the NMR data is quite poor and very succinct, key points regarding the structural elucidation of AT LEAST the glycerol/butanetriol moieties deserving to be argued in much greater details (e.g., the methyl group C4' should be present as a doublet. Is it the case? If so, what is the value of the coupling constant?). What kind of correlations proving the proposed structure can be used from the 2D NMR experiments? In the present state, strictly no arguments are provided to justify the proposed structure, and notably why the extra methyl group is located at C-3' and not elsewhere. Since this identification is of prime importance in the sense that it describes a novel compound series (cf. the title of the manuscript), more work is needed (see the paper from Sinninghe Damsté et al., 2002 in Journal of Lipid Research as an excellent example of NMR description for such complex compounds). Figures illustrating some key features could be added, either to the main manuscript, or as supplementary material.

In agreement with the suggestions by Reviewer 1, we expanded the description of the NMR result part to describe key correlations (cf. excerpt below) and also added notes to Table 1 as an additional column. We now include three new supplementary figures including (i) 1D ^1H spectra, (ii) plots of two regions from the 2D ^1H - ^{13}C HSQC spectra and (iii) expansions from the same regions in the 2D ^1H - ^{13}C HMBC spectra. Note the multiplicity editing used in the ^1H - ^{13}C HSQC spectra that assists enormously in distinguishing the glycerol/butanetriol moieties and their unique distribution of methyl/methine and methylene signals. The lack of reported J-coupling constants was not an omission. We now include a 1D spectrum (as supplementary figure) which makes it much clearer that there is severe overlap in the 1D ^1H dimension that precluded reliable extraction of coupling constants (the desymmetrisation of BDGT-0 compared to GDGT-0 leads to extensive overlap). We include several other J-coupling constant values but with cautionary notes to the table. This includes the C4' methyl group that is an overlapped doublet.

Proposed modifications for the NMR result part: "Analysis of high-resolution ^1H and ^{13}C one-dimensional spectra revealed a number of downfield signals (3.15-3.70 ppm) that suggested desymmetrization when compared to the expected number of signals from, for example, GDGT-0 (Supplementary Figure 1; Sinninghe Damsté et al., 2002). Analysis of two-dimensional spectra (^1H - ^{13}C HSQC and HMBC, ^1H - ^1H COSY and TOCSY, Table 1) revealed one set of ^1H and ^{13}C chemical shifts closely matching the assignments of the glycerol components and ether linked CH_2 groups of GDGT-0 (Table 1; Sinninghe Damsté et al., 2002). These included the characteristic methine signal of C2 and methylene signals of C1 and C3 (Supplementary Figure 2B) that could be connected via HMBC correlations (e.g. C1 correlated to C2 and C3) and ^1H connectivities. The resolved diastereotopic protons 3.68 ppm to 3.58 ppm (C1 protons), 3.51 and 3.44 ppm (C3 protons) and 3.49 (C2 proton) also confirmed these

assignments. C3 could be correlated with A1 via ^1H - ^{13}C HMBC correlations through the ether linkage (Supplementary Figure 3) and A1 and B1 were linked to A2/A3 and B2 respectively also via HMBC.

However, a number of new O-linked methine (C2' and C3') and methylene signals (A1', B1' and C1') were visible compared to ^1H - ^{13}C HSQC spectra of GDGT-0 as well as an additional aliphatic methyl signal (C4', 16.62 ppm; Supplementary Figures 1-3). The strong C4' signal appeared as a doublet in the 1D ^1H spectrum (Supplementary Figure 1), albeit overlapped and consistent with coupling to the single C3' methine proton. C4' showed clear correlations via HMBC to both C3' and C2' (Supplementary Figure 3, annotated) and well-resolved ^1H correlations in the ^1H - ^1H COSY/TOCSY spectra to the C1', C2' and C3' protons. The characteristic downfield ^{13}C shift of C2' also gave resolved correlations to C1' and C3'. C2' and C3' could then be correlated via HMBC through their ether linkages to resolved O-linked CH_2 signals (A1' and B1'). Similarly, A1' and B1' could be correlated to A2' and B2' respectively as both were partially resolved from A2 and B2. A3/3' and B3/3' appeared to give a single methine resonance in the ^1H - ^{13}C HSQC spectrum but were partially resolved in the ^1H - ^{13}C HMBC, showing A3 and A3' could be distinguished by their ^{13}C chemical shifts (29.71 and 29.54 ppm respectively) and were resolved from B3/3' (29.60 ppm). Aside from this, the remainder of the (highly overlapped) branched alkyl chain chemical shifts (from A4'/B4' onwards, Supplementary Figure 2A) were superimposable on those of GDGT-0 suggesting an identical arrangement of branched methyl groups (Table 1). Together these analyses confirmed the presence of a butanetriol group at the opposing end of the molecule (Fig. 2) and four resolvable ether linkages."

A second point deals with the possible biological origin(s) of the BGDs and PDGs. According to the authors, and given the $\delta^{13}\text{C}$ values of bp-0 released upon ether cleavage/hydrogenolysis of isolated IPL BGD-0 and IPL GDGT-0, as compared to the $\delta^{13}\text{C}$ values of CH_4 , TOC and DIC in different sedimentary settings, BGD-0 shows a $\delta^{13}\text{C}$ composition systematically more ^{13}C enriched than CH_4 . As pointed out by the authors, this indicates that the microorganisms producing BGDs (and PGDs) are not methanotrophs. It is then suggested that the $\delta^{13}\text{C}$ values determined for bp-0BGD in the Black Sea and Rhone delta may be indicative of methanogens, whereas other source organisms with a different metabolism may produce BGDs in the other settings. From the data presented, I agree that a methylotrophic source for BGDs can be ruled out, but this is more or less all that can be deduced from the $\delta^{13}\text{C}$ values. Mixed sources (instead of methanogens) cannot be excluded in the case of the Black sea and Rhone delta sediments (methane itself likely originates from different producers), and a methanogenic origin cannot be ruled out in the case of the other sediment settings (cf. discussion from lines 240 to 252). From the abstract (lines 18-22), these possibilities in the different setting are presented as being more "clear-cut" as they really are. This should perhaps be reworded (in the abstract).

In agreement with the comment by Reviewer 1, we modified the abstract (see below) to better match our discussion of potential biological sources BDGs and PDGs.

Proposed modification of the abstract: "We further systematically explored the abundance, distribution and isotopic composition of BDGs and PDGs as both intact polar and core lipid forms in marine sediments collected in contrasting environments of the Mediterranean Sea and Black Sea. High proportions of intact polar BDGs and PDGs in the deeper methane-laden sedimentary layers and relatively ^{13}C -depleted BDGs, especially in the Rhone delta and in the Black Sea, are in agreement with a probable methanogenic source for these lipids. However, contributions from heterotrophic archaea to BDGs (and PDGs) cannot be excluded, particularly in the eastern Mediterranean Sea, and contrasting BDG and PDG headgroup distribution patterns were observed between the different studied sites. This points to additional, non-methanogenic, archaeal sources for these lipids."

In addition to these two main points, there are a few minor corrections (typos, mainly) to make.

- Lines 18-22 (abstract): see previous comments about mixed sources in the Black sea and Rhone delta sediments

The abstract was changed accordingly (see previous comment).

- Line 123: DCM at 60 °C? In a sealed tube? Please specify.

The sentence was modified accordingly.

- Line 129: Is the second decimal value (0.03‰ meaningful in the case of d13C measurements?

The sentence was modified as follows: "Every sample was measured in duplicate and the associated error was lower or equal to 1‰."

- Line 131: replace "analysis" by "composition".

The sentence was modified accordingly.

- Line 168: "high-resolution one and twodimensional...". See also general comments for section 3.1, in which the NMR data (of the butanetriol moiety, at least) should be discussed in much greater details.

As detailed in our answer to the reviewer's general comment, we expanded the discussion of the NMR data.

- Line 288: replace "side-chains" by "isoprenoid chains".

The sentence was modified accordingly.

- Line 288: If I'm right, in Elling et al., the extra methyl group reported is located on the glycerol moiety ("MeO-Archaeol") and not on the isoprenoid chain.

Indeed, Reviewer 1 is right. We modified the sentence as follows to be more specific:

"Additional methylations have been previously observed on the isoprenoid chains or as methoxylation on the glycerol in different lipid classes (e.g. Elling et al., 2017; Knappy et al., 2015)"

- Line 298: "butanetriol- or pentanetriol-based"

The sentence was modified accordingly.

- Lines 324-326: "suggesting a distinct role in the cell membranes". What do the authors mean by this? Given the structure of BGDs (hydrophilic head groups and hydrophobic isoprenoid chains), it is difficult to conceive a distinct role than "classical" GDGs... And what is the relationship between the differences in the d13C composition of BGDs and GDGs and the membrane role? The differences in stable carbon isotopic composition can be attributed to different microorganisms producing BGDs and GDGs and having different metabolisms.

This sentence was indeed not clear. We have decided to delete it as it was not adding substantial information to the conclusion.

- Line 364: *Methanomassiliicoccus luminyensis*: in italics

The sentence was modified accordingly.

- Line 365: add volume number (82) and page numbers (4505-4516) - Line 383: De Rosa - Line 405: replace "802" by "802-805" - Line 410: Add page numbers (3090- 3095) after 63, and delete "6" - Line 431: *Candidatus*: in italics - Line 469: D14C - Line 469: delete "15" and add page numbers (3123-3137)

The reference list was modified accordingly.

- Table 1: To be revised and completed according to the first main comment.

The table was modified accordingly (cf. response on reviewer's general comments).

- Figure 5 (caption), Line 558: add "between dissolved CO₂ and DIC, considering..." after - 10.7‰

The sentence was modified accordingly.

Response to Darci Rush:

This paper by Coffinet et al., entitled “Structural elucidation and environmental distributions of butanetriol and pentanetriol dialkyl glycerol tetraethers (BDGTs and PDGTs)” employs 2-dimensional nuclear magnetic resonance (2D-NMR) to confirm the structure of a previously unconfirmed lipids: BDGT. Furthermore, by investigating the ^{13}C isotopic composition of biphytanes originating from these lipids in marine sediments, and comparing them with potential carbon sources (CH_4 , TOC, DIC), the authors go on to suggest potential source organisms, or rather carbon metabolisms, of these lipids.

The authors do well in not over-interpreting their environmental results. They speculate that BDGTs and PDGTs likely are produced by a diverse archaeal community, and not just one confirmed synthesizer, the methanogen *Methanomassiliicoccus luminyensis*. I appreciate that they go on to suggest why these lipids may be found in such a range of archaea: BDGTs and PDGTs might boost membrane stability under low energy conditions found in deep sediments. Overall, I find this to be a useful paper for the community in general, and worthy of publication in Biogeosciences.

There are a couple of points that I would like the authors to address, however. I find the structural elucidation of BDGT-0 to be the most important aspect of this study. Far too few NMR experiments are performed in organic geochemistry, as these involve a lot of effort and lab hours and often we do not have enough starting material. I appreciate that the authors took the time to undertake the work here. However, I feel that they are doing themselves a disservice by not publishing the 2D correlation results of these experiments. They report having performed COSY, TOCSY, HMBC, and HSQC experiments. I suggest including at least a couple of these in Table 1. For example, they refer to the HMBC and HSQC results (line 171) confirming a butanetriol end group, and for clarity/transparency, I feel it would be useful to have these included in Table 1.

We agree with Darci Rush and added those results, which allowed us to confirm the butanetriol backbone, in Table 1 as an additional column. As also detailed above in our response to Reviewer 1, we considerably expanded the description of the NMR analysis.

Furthermore, for some of the most important hydrogen shifts at the very least, I suggest that they also include the coupling constants (J) and multiplicities, especially for those of the “C” carbons, which are the unusual components of this molecule.

There is severe overlap in the 1D ^1H dimension that precluded reliable extraction of coupling constants (the de-symmetrisation of BDGT-0 compared to GDGT-0 leads to extensive overlap). This is the reason why we did not report J-coupling constants. Nevertheless, we now include a 1D ^1H spectrum as a supplementary figure, which clarifies this point. We also include several other J-coupling constant values with cautionary notes to the table. This includes the C4' methyl group that is an overlapped doublet.

Finally, the number of significant figures on the hydrogens associated with A4, A4' etc is more (i.e. 1.022 – 1.105) than for that of all the other reported hydrogen shifts. Why is this? I also found a couple of lost 0s in the table (likely an artifact of program used to generate the table).

We thank Darci Rush for spotting this and have corrected significant figures and formatting issues. Table 1 was modified to enhance clarity.

Minor comments:

Line 9: Czech Republic?

The Czech government adopted “Czechia” as the official name of the country in English in 2016 and this is consistent with the designation by the UN’s database for official country names (cf. United Nations Group of

Experts on Geographical Names, UNGEGN List of Country Names (New York: United Nations, 2017) available from unstats.un.org/unsd/geoinfo/UNGEgn/docs/11th-uncsgn-docs/E_Conf.105_13_CRP.13_15_UNGEgn%20WG%20Country%20Names%20Document.pdf.

Line 29: Consider replacing amphiphilicity with “amphiphilic nature”

Line 31: sn should be in italics

Line 52: lipids

Line 52: currently the only

Line 55: capacity change to capability

Line 134: as follows

Line 261: , as well as the absence of PDGTs

Line 264: a higher relative

Sentence starting line 317: There are two “therebys” in this sentence. Consider removing one.

Line 327: Thus, it seems likely

Caption for Figure 5: The last sentence should mention that the calculation of $\delta^{13}\text{CCO}_2$ using the fractionation - 10.7‰ comes from the measured values of DIC. This is clear in the text, but not here.

These comments were all taken into account in the revised manuscript.

Structural elucidation and environmental distributions of butanetriol and pentanetriol dialkyl glycerol tetraethers (BDGTs and PDGTs)

Sarah Coffinet¹; Travis B. Meador^{1,*}; Lukas Mühlena¹; Kevin W. Becker^{1,**}; Jan Schröder¹; Qing-Zeng Zhu¹; Julius S. Lipp¹; Verena B. Heuer¹; Matthew P. Crump²; Kai-Uwe Hinrichs¹

5 ¹MARUM – Center for Marine Environmental Sciences, University of Bremen, Germany

²School of Chemistry, University of Bristol, United Kingdom

Correspondence to: Sarah Coffinet (scoffinet@marum.de)

Present addresses:

* Biology Centre CAS, SoWa-RI, České Budějovice, Czechia

10 ** GEOMAR Helmholtz Centre for Ocean Research, Kiel, Germany

Abstract. Butanetriol and pentanetriol dialkyl glycerol tetraethers (BDGTs and PDGTs) are membrane lipids recently discovered in sedimentary environments and in the methanogenic archaeon *Methanomassiliicoccus luminyensis*. They possess an unusual structure, which challenges fundamental assumptions in lipid biochemistry. Indeed, they bear a butanetriol or a pentanetriol backbone instead of a glycerol at one end of their core structure. In this study, we unambiguously located the additional methyl group of the BDGT compound on the C3 carbon of the lipid backbone via high-field ~~two-dimensional~~ NMR experiments. We further systematically explored the abundance, distribution and isotopic composition of BDGTs and PDGTs as both intact polar and core lipid forms in marine sediments collected in contrasting environments of the Mediterranean Sea and Black Sea. High proportions of intact polar BDGTs and PDGTs in the deeper methane-laden sedimentary layers and, in addition, relatively ¹³C-depleted BDGTs, especially from in the Rhone delta and from in the Black Sea, are in agreement with a probable methanogenic source for these lipids. In line with this interpretation, high proportions of intact polar BDGTs and PDGTs were detected in the deeper methane-laden sedimentary layers. However, contributions from heterotrophic archaea to BDGTs (and PDGTs) cannot be excluded, particularly in the eastern Mediterranean Sea, and relatively ¹³C-enriched BDGTs and contrasting BDGT and PDGT headgroup distribution patterns were observed of BDGTs and PDGTs in between the different studied sites. This points to additional, non-methanogenic, sediments of the Eastern Mediterranean Sea imply that additional archaeal groups also produces these unique lipids for these lipids.

1 Introduction

Unique membrane lipids were a key argument to postulate the existence of Archaea as a third and independent domain of life, as distantly related to Bacteria as to Eukarya, when Woese et al. (1990) proposed their revised tree of life. Membrane lipids form an envelope that separates cells from their environment and protects their interior components. Specific chemical properties define the fluidity and permeability of the membrane barrier, regulating what can enter the internal cell compartment. On the one hand, membrane lipids from members of all domains of life share some common characteristics, such as their amphiphilicity/amphiphilic nature. That is, they all possess apolar alkyl chains and polar headgroups held together by a glycerol moiety (Lombard et al., 2012). On the other hand, membrane lipids of Archaea fundamentally differ from those of Bacteria and Eukarya in that they contain (bi)phytanyl chains constituted from the condensation of several isoprenoid units and ether linkages to the *sn*2 and *sn*3 carbons of a glycerol backbone (De Rosa and Gambacorta, 1988; Koga and Morii, 2005). On the contrary, Bacteria and Eukarya generally produce fatty acyl chains linked to the *sn*1 and *sn*2 carbons of the glycerol backbone (Kates, 1977). Intensive exploratory analyses of lipid extracts from pure cultures and environmental samples over the last decades (e.g. Elling et al., 2017; Koga et al., 1993; Koga and Morii, 2005; Liu et al., 2012; Meador et al., 2014; Paściak et al., 2003; Schouten et al., 2000, 2013; Sturt et al., 2004; Weijers et al., 2006), revealed a large diversity of membrane lipids and a

40 more complex picture than first considered by Woese et al. (1990). Several non-isoprenoid ether glycerol lipids were identified as of bacterial origin, such as the branched glycerol dialkyl glycerol tetraethers (brGDGTs, Weijers et al., 2006) or the alkyl glycerol ether lipids (AGEs; e.g. Hinrichs et al., 2000; Pancost et al., 2001; Rütters et al., 2001). To date, AGEs have been observed in a wide range of pure cultures, covering different bacterial phyla with contrasting physiologies (Vinçon-Laugier et al., 2016). In addition, lipids containing both a (bi)phytanyl and a non-isoprenoidal alkyl chain were previously observed in
45 natural environments (Liu et al., 2012; Schouten et al., 2000). Nevertheless, all the above-mentioned membrane lipids possess glycerol backbones, which appear to be a common feature shared by members of all domains of life.

The recent identification of butanetriol and pentanetriol dialkyl glycerol tetraethers (BDGTs and PDGTs, Knappy et al., 2014; Zhu et al., 2014), in which one glycerol is substituted by a butanetriol or pentanetriol, challenges this assumption. Tandem mass spectrometry complemented with gas chromatography (GC) detection of butanetriol after hydrolysis (Zhu et al., 2014)
50 demonstrated the presence of a 1,2,3 butanetriol backbone in BDGTs but did not specify its configuration within the lipid molecule, notably its linkages with the biphytanyl side chains. Subsequently, BDGTs and PDGTs were observed in diverse samples, both as intact polar lipids (IPLs, lipids with polar headgroups) and core lipids (CLs, lipids without polar headgroups), from recent organic-rich estuarine sediments (Meador et al., 2015) to old Jurassic marine shales (Knappy et al., 2014) and deep subsurface sediments (Becker et al., 2016; Zhu et al., 2014). Furthermore, Becker et al. (2016) identified BDGTs as prominent
55 membrane lipids in *Methanomassiliicoccus luminyensis*, ~~the~~ currently the only cultured representative of the seventh order of methanogens; lower quantities of PDGTs were also observed in this archaeon. BDGTs accounted for up to 82% of the detected core lipids, while being absent from 25 different pure cultures spanning the main archaeal phyla and encompassing several representatives of the different orders of methanogens, thus leading to the conclusion that the capacity-capability to synthesize BDGTs and PDGTs among the methanogens could potentially be restricted to the order Methanomassiliicoccales (Becker et al., 2016). However, this exclusive chemotaxonomic relationship contrasts with the wide diversity of geochemical settings
60 where BDGTs and PDGTs have been detected and cultured representatives for several archaea phyla remain unavailable for screening. For example, Meador et al. (2015) had suggested members of the Miscellaneous Crenarchaeotal Group, now termed Bathyarchaeota, as a source of BDGTs in the estuarine White Oak River Basin due to the similarly high relative abundances and correlation of BDGTs with bathyarchaeotal 16S genes in the sediment profile.

65 In the present study, the exact structure of the core BDGT molecule was elucidated through high-field two-dimensional NMR analysis of BDGT purified from a pure culture of *M. luminyensis*. In addition, the relative abundance of BDGTs and PDGTs and stable carbon isotopic composition ($\delta^{13}\text{C}$) of BDGTs were systematically investigated in a set of 48 marine sediment samples covering a wide range of environmental and geochemical conditions. Our aim was to provide new insights into the diversity and carbon metabolism of BDGT and PDGT producers and on the potential roles of these novel lipids in the cell
70 membrane.

2 Material and Methods

2.1 Sample collection

Marine sediment samples were collected with a combination of multi-corer and gravity coring at eight different sites (Fig. 1) in the Mediterranean and Black Seas during two expeditions: RV *Meteor* Cruise M84/1 (Zabel et al., 2011) and RV *Poseidon*
75 Cruise POS450 (Heuer et al., 2014). Description of the environmental characteristics, geochemical and sedimentary conditions of the eight visited sites can be found in Schmidt et al. (2017). From these locations, 48 samples spanning different environments and geochemical conditions were selected for detailed organic geochemical investigation (Suppl. Table 1).

2.2 Marine sediment lipid extraction and quantification

Lipid extraction of sediment samples was performed according to a modified Bligh & Dyer method (Sturt et al., 2004). All frozen sediment samples were homogenized at -196°C using a CryoMill (Retsch), which was operated as follows: two cycles of pre-cooling for 2 min each, with a speed of the impactor of 5 impacts s^{-1} and homogenizing and fragmenting for 2 min with 25 impacts s^{-1} . Samples (ca. 50-60 g wet weight) were then lyophilized and ultrasonically extracted four times with a mixture of DCM/MeOH/buffer (1:2:0.8; v:v:v), with a phosphate buffer at pH 7.4 for the first two steps and a trichloroacetic acid buffer at pH 2.0 for the remaining two steps. The sample was extracted in two final steps with DCM/MeOH (5:1). Each extraction step was followed by centrifuging the samples for 10 min and the resulting supernatants were combined in a separatory funnel. An equal amount of DCM and Milli-Q water was added to the supernatants and the separatory funnel was thoroughly mixed. After phase separation the aqueous phase was washed three times with DCM and the water phase was discarded. The organic phase was washed three times with Milli-Q water, collected and evaporated to dryness under a stream of N_2 . The total lipid extracts (TLE) obtained were stored at -20°C until further analysis.

Detection and quantification of intact polar lipids (IPLs) were carried out on a maXis plus ultra-high resolution quadrupole-time-of-flight mass spectrometer (Q-ToF-MS; Bruker), coupled to an Ultimate 3000RS ultra high pressure liquid chromatography instrument (UHPLC; Dionex). IPLs were chromatographically separated by an ACE3 C18 column (150 x 2.1 mm; particle size 3 μm ; ACE) as described by Zhu et al. (2013) and detected in positive ionization mode scanning a mass range of 150 – 2000 Da. Lipids were identified by retention time, exact mass (± 0.001 Da), and characteristic fragmentation patterns obtained by data-dependent MS^2 scans. IPLs were quantified by comparison of the intensity of parent ions with that of a C_{46} -glycerol trialkyl glycerol tetraether (GTGT; Huguet et al., 2006) added as an internal standard. IPL concentrations were corrected for their response factors determined from purified and commercially available standards following the procedure described by Becker et al. (2016).

2.3 Stable carbon isotope analysis

Six of the 48 marine sediment TLE from the Rhone delta, the eastern Mediterranean Sea and the Black Sea (Samples # 5, 8, 20, 22, 34, 38 of the dataset; detailed information available in Suppl. Table 1) were selected to investigate the natural stable isotopic composition of the BDGT-derived biphytanes. Only IPL-BDGTs were analyzed as they are more likely to derive from living organisms. Before isotopic analysis via gas chromatography coupled to isotope ratio mass spectrometry (GC-IRMS), IPL-BDGTs were purified with two steps of preparative HPLC and then cleaved into biphytanes (bp), as detailed below.

2.3.1 Preparative HPLC

TLE samples were first separated into IPL and CL fractions by preparative HPLC (Agilent 1200 series) with a modified version of the protocol reported by Meador et al. (2015). TLE separation was performed on an LiChrospher Diol column (250 x 10 mm; 5 μm , Grace) with *n*-hexane/isopropanol (90:10; v/v) as eluent A and 100% isopropanol as eluent B. Chromatographic conditions were as follows: a gradient from 100% A at 3 ml min^{-1} to 24% B in 15 min and then to 100% B in 5 min at a flow rate of 2 ml min^{-1} . 100% B at 2 ml min^{-1} was maintained for 10 min before switching back to the initial conditions for 15 min. During the run, the eluent flow was split (split ratio 150:1; Agilent active splitter G1968D) between the fraction collector and an online mass spectrometer (Agilent 6130 single quadrupole) allowing continuous monitoring of retention time stability. Fraction 1 (F1), containing the CLs, was collected from 0 to 7 min and fraction 2 (F2), containing the IPLs, from 11 to 30 min. The collected fractions were subsequently dried under a stream of N_2 . IPLs were then converted into CLs by acid hydrolysis with 1 M ~~HCL~~-HCL in MeOH for 3 h at 70°C (Pitcher et al., 2009; Elling et al., 2014).

CL-BDGTs were further separated from CL-GDGTs according to Zhu et al. (2014). The hydrolyzed IPL fraction was injected into an Agilent 1200 normal phase HPLC-system equipped with a PerfectSil CN-3 column (250 x 10 mm, 5 μm , MZ Analysentechnik). Separation was achieved at a flow rate of 2.5 ml min^{-1} with an elution gradient from 100% A (99:1 *n*-

hexane:isopropanol) held for 5 min, ramping to 10% B (90:10 *n*-hexane:isopropanol) at 12 min and then to 100% B at 30 min finally holding 100% B for 12 more min. The solvent system was then returned to initial conditions for 10 min. Retention time stability was monitored via simultaneous MS detection as above. BDGTs and GDGTs were collected between 13 and 16 min and between 16 and 21 min, respectively.

2.3.2 Ether cleavage and compound specific stable carbon isotope analysis

Ether cleavage with BBr₃ was performed on the purified CL-BDGT and CL-GDGT fractions to convert them into biphytanes (bp) following the protocol by Kellermann et al. (2012). Briefly, aliquots of the dried fractions were amended with 200 µl of 1 M BBr₃ dissolved in DCM and incubated in sealed tubes at 60 °C for 2 h followed by reduction with 200 µl of 1 M superhydride in tetrahydrofuran. Liquid-liquid extraction with H₂O and *n*-hexane was performed three times and the aqueous phase was discarded. The apolar phase was purified on a silica column with *n*-hexane as eluent. Carbon isotopic composition of biphytanes was measured on a Trace GC Ultra coupled to a GC-IsoLink ConFlow IV interface and a Delta V Plus IRMS (Thermo) equipped with a Rxi-5ms column (30 m x 250 µm x 0.25 µm, Restek). The injection temperature was set at 300 °C; the initial oven temperature was held at 60 °C for 1 min, followed by an increase to 150 °C at 10 °C min⁻¹ and then to 320 °C at 4 °C min⁻¹ with a flow rate of 1.2 ml min⁻¹. Every sample was measured in duplicate and the associated error ranged between 0.03‰ and was lower or equal to -1‰.

2.4 Stable carbon isotope analysis composition of potential carbon sources

In order to gain information on the C sources of BDGTs, the stable carbon isotope analysis of the total organic carbon (TOC), the dissolved inorganic carbon (DIC) and methane (CH₄) was determined. TOC content and stable carbon isotopic analysis ($\delta^{13}\text{C}_{\text{TOC}}$) was-were previously described in Schmidt et al. (2017). Stable carbon isotopic compositions analysis of DIC ($\delta^{13}\text{C}_{\text{DIC}}$) and CH₄ ($\delta^{13}\text{C}_{\text{DIC}}$, $\delta^{13}\text{C}_{\text{CH}_4}$) were measured on shore within the year following each cruise. Prior to analysis, pore water aliquots of 2 ml were stored at -20 °C in vials without headspace for $\delta^{13}\text{C}_{\text{DIC}}$ analysis and ca. 3 ml of sediment were stored at 4 °C in 22 ml gas tight vials amended with 5 ml NaOH for $\delta^{13}\text{C}_{\text{CH}_4}$ analysis. $\delta^{13}\text{C}_{\text{DIC}}$ was measured using a gas bench coupled to a Finnigan MAT 252 mass spectrometer. Samples were prepared as follows: 100 µl of phosphoric acid were transferred to glass tubes, which were subsequently sealed with butyl septa and plastic caps and purged five times with helium. Fluid samples (0.2–1.0 ml) were injected into the purged tubes by syringe and allowed to degas CO₂ from the acidified aqueous matrix for at least five hours. Carbon isotopic compositions of CO₂ were then analyzed in subsamples of the gas phase. The precision of the analysis was 0.1‰ (1σ). CH₄ stable carbon isotope values were determined on a Trace GC Ultra coupled to a GC combustion III interface and a Delta Plus XP IRMS (Thermo) equipped with a Carboxen 1006 Plot column (Supelco, Sigma Aldrich). Injection temperature was set at 200 °C, the oven temperature was held at 40 °C for 6 min and the flow rate at 3 ml min⁻¹.

2.5 Cultivation of *Methanomassiliicoccus luminyensis*, lipid extraction and BDGT-0 purification for NMR analysis

M. luminyensis strain was purchased at DSMZ (Leibniz Institute DSMZ – German Collection of Microorganisms and Cell Cultures) and grown in an anaerobic medium optimized by the DSMZ (protocol 1637). A total volume of 2 l of culture was grown in two 2 l Schott bottles, inoculated with 10% (v/v) of a previous culture grown under the same conditions, i.e. at 37 °C under an atmosphere containing 80% H₂ and 20% CO₂. After 16 days, cells were harvested by centrifugation (25 min; 4500 rpm) and were subsequently lyophilized.

Direct acid hydrolysis of the freeze-dried biomass pellet was performed according to Becker et al. (2016) using 1 M HCl in MeOH for 16 h at 70 °C. CLs were extracted by ultra-sonication (two times 20 min) with a 5:1 DCM:MeOH solvent mix and the extracts were collected in a separatory funnel. Lipids were partitioned into the organic phase following addition of Milli-Q H₂O. The water phase was then extracted three times with an equal amount of DCM. The organic phases were pooled in an

Erlenmeyer flask before transfer into the separation funnel and further washing (three times) with an equal amount of Milli-Q H₂O. The water phase was discarded and the organic solvent was evaporated under a gentle flow of N₂. CL-BDGT-0 was purified by preparative HPLC following the same preparative HPLC protocol as described in Section 2.3.1. BDGT-0 was collected between 12.3 and 13 min. BDGT-0 was estimated to be pure at 99.4% via UHPLC-QToF-MS following the protocol by Becker et al. (2015).

2.6 NMR analysis

BDGT-0 (860 µg) was dissolved in CDCl₃ (170 µL) and transferred to a 3 mm NMR tube. ¹H, ¹³C spectra and two-dimensional COSY, TOCSY, ¹H-¹³C HSQC and ¹H-¹³C HMBC were acquired at 600 MHz on a Varian VNMRs spectrometer equipped with triple resonance ¹H observe cryogenic probe. Spectra were processed and analyzed using VnmrJ 4.2 software provided with the spectrometer.

2.7 Statistical analysis

Principal component analysis (PCA) was performed with the R software using factominR and vegan packages. PCA requires all variables to follow a normal distribution, thus all data were reduced and centered before analysis.

3 Results

3.1 NMR analysis of BDGT-0 extracted from *M. luminyensis*

Analysis of high-resolution ¹H and ¹³C one-dimensional spectra revealed a number of downfield signals (3.15-3.70 ppm) that suggested desymmetrization when compared to the expected number of signals from, for example, GDGT-0 (Supplementary Figure 1; Sinninghe Damsté et al., 2002). Analysis of two-dimensional spectra (¹H-¹³C HSQC and HMBC, ¹H-¹H COSY and TOCSY, Table 1) revealed one set of ¹H and ¹³C chemical shifts closely matching the assignments of the glycerol components and ether linked CH₂ groups of GDGT-0 (Table 1; Sinninghe Damsté et al., 2002). These included the characteristic methine signal of C2 and methylene signals of C1 and C3 (Supplementary Figure 2B) that could be connected via HMBC correlations (e.g. C1 correlated to C2 and C3) and ¹H connectivities. The resolved diastereotopic C1 protons 3.68 ppm to 3.58 ppm (C1 protons), 3.51 and 3.44 ppm (C3 protons) and 3.49 (C2 proton) also confirmed these assignments. Multiplicity editing (opposite signal phases for methyl/methine and methylene signals) applied in the ¹H-¹³C HSQC spectra assisted in this assignment and in distinguishing the glycerol/butanetriol moieties and their unique distribution of methyl/methine and methylene signals as detailed below. C3 could be correlated with A1 via ¹H-¹³C HMBC correlations through the ether linkage (Supplementary Figure 3) and A1 and B1 were linked to A2/A3 and B2 respectively also via HMBC. However, a number of new ¹H-¹³C HSQC spectra of GDGT-0 as well as an additional aliphatic methyl signal (C4', 16.62 ppm; Supplementary Figures 1-3). The strong C4' signal appeared as a doublet in the 1D ¹H spectrum (Supplementary Figure 1), albeit overlapped and consistent with coupling to the single C3' methine proton. C4' showed clear correlations via HMBC to both C3' and C2' (Supplementary Figure 3, annotated) and well-resolved ¹H correlations in the ¹H-¹H COSY/TOCSY spectra to the C1', C2' and C3' protons. The characteristic downfield ¹³C shift of C2' also gave resolved correlations to C1' and C3'. C2' and C3' could then be correlated via HMBC through their ether linkages to resolved O-linked CH₂ signals (A1' and B1'). Similarly, A1' and B1' could be correlated to A2' and B2' respectively as both were partially resolved from A2 and B2. A3/3' and B3/3' appeared to give a single methine resonance in the ¹H-¹³C HSQC spectrum but were partially resolved in the ¹H-¹³C HMBC, showing A3 and A3' could be distinguished by their ¹³C chemical shifts (29.71 and 29.54 ppm respectively).

and were resolved from B3/3' (29.60 ppm). Aside from this, the remainder of the (highly overlapped) branched alkyl chain chemical shifts (from A4'/B4' onwards, Supplementary Figure 2A) were superimposable on those of GDGT-0 suggesting an identical arrangement of branched methyl groups (Table 1). - The HSQC and HMBC connectivity confirmed these signals to belong to a Together these analyses confirmed the presence of a butanetriol group at the opposing end of the molecule (Fig. 2) and four resolvable ether linkages. Further desymmetrization compared to GDGT-0 led to distinguishable ether-linked CH₂ signals (A1' and B1') and partial resolution of A2 and A2'. Aside from this, the remainder of the branched alkyl chain chemical shifts were superimposable on those of GDGT-0 suggesting an identical arrangement of branched methyl groups (Table 1).

3.2 BDGT and PDGT in the Mediterranean and Black Sea sediments

3.2.1 BDGT and PDGT abundance and diversity

Geochemical parameters of the 48 analyzed samples were previously described in Schmidt et al. (2017). Notably, TOC values ranged between 0.08 and 4.37% (Suppl. Table 1). The highest TOC content was measured in the sapropel layers of the eastern Mediterranean Basin (GeoB15103) while the basin sites, i.e. eastern Mediterranean Basin (excluding the sapropel layers), Cap de Creus Canyon and Ligurian-Provençal Basin (GeoB15103, GeoB17302, GeoB17304), exhibited the lowest TOC contents. From the 48 samples, ranging in depth from surface to 635 cm and ages from modern to ~173,000 years, BDGTs and PDGTs were detected as CLs and IPLs in 45 and 37 samples, respectively. PDGTs were not detected in samples from the Black Sea (GeoB15105). Concentrations ranged from 0.04 to 9.2 µg g⁻¹ C_{org} for BDGTs and from 0.04 to 3.1 µg g⁻¹ C_{org} for PDGTs, which correspond, in average, to 8 and 3% of the GDGT-0 concentration in these samples, respectively (Suppl. Table 2). BDGT structures with up to 2 cycloalkyl rings were assigned based on their retention time and MS² spectra but BDGT-0 was generally predominant (Suppl. Table 2). IPL-BDGTs and IPL-PDGTs comprised mono- (1G) and diglycosidic (2G) lipids. The relative abundance of these IPLs within the total pool comprised of both the corresponding CLs and IPLs (on average, 74% for IPL-BDGTs and 93% for IPL-PDGTs) was much higher than the relative abundance of IPL-GDGTs (18% on average; Suppl. Table 2 and Fig. 3).

3.2.2 Principal Component Analysis (PCA) on BDGT and PDGT distribution

In order to evaluate the variability in BDGT and PDGT distribution within the dataset, a PCA was performed with the major environmental variables and indices of BDGT and PDGT relative abundances. In addition to the fractional abundance for each BDGT and PDGT pool [$f(\text{CL-BDGTs})$, $f(\text{1G-BDGTs})$, $f(\text{2G-BDGTs})$, $f(\text{CL-PDGTs})$, $f(\text{1G-PDGTs})$, $f(\text{2G-PDGTs})$], the relative proportion of IPLs to the total lipid content [$f(\text{IPL-BDGTs})$, $f(\text{IPL-PDGTs})$] and the relative proportion of BDGTs and PDGTs to the total GDGT-0 content [(sum-BDGTs)/(sum-GDGT-0), (sum-PDGTs)/(sum-GDGT-0)] were computed (Suppl. Table 2). This PCA separated three groups of samples that differed from their geochemical properties and their BDGT and PDGT content (Fig. 4). The first group contained all samples from the Rhone delta (sites GeoB17306, 7, 8) and is characterized by high concentrations of dissolved Fe and CH₄, shallow water depths, and relatively low values of δ¹³C_{TOC} (Fig. 4). This sample group shows a high proportion of BDGTs and PDGTs relative to GDGT-0, and a high proportion of IPL-BDGTs and IPL-PDGTs, especially as diglycosidic lipids (2Gs; Fig. 4). The second group of samples includes all samples collected in the Black Sea (GeoB15105), with high concentrations of DIC, DOC, and HS⁻, and a low concentration of SO₄²⁻. The last group comprises all samples from basin sites, which are characterized by relatively lower TOC and lower terrestrial input, i.e. from the eastern Mediterranean basin (GeoB15103), the Marmara Sea (GeoB15104) and Cap de Creus and Ligurian-Provençal Basin (GeoB17302 and 17304). These samples all exhibit high water depth, less negative δ¹³C_{TOC} values and higher concentrations in SO₄²⁻. The Black Sea and basin site groups are characterized by higher contributions of CL- and 1G-BDGTs than the first group of river delta samples. Moreover, the Black Sea group differs from the other groups by its high proportion of CL-BDGTs and its lack of PDGTs (both CL and IPL) while the basin sites are relatively enriched in 1G-PDGTs (Fig. 4).

3.2.3 Stable carbon isotopic composition of BDGT-0

Six samples were selected for analysis of the ^{13}C isotopic composition ($\delta^{13}\text{C}$) of the IPL-BDGT derived biphytanes. A dedicated preparative LC protocol enabled comparison of $\delta^{13}\text{C}$ of bp-0 from IPL-BDGT-0 ($\delta^{13}\text{C}_{\text{BDGTs}}$) with that derived of bp-0 from IPL-GDGT-0 ($\delta^{13}\text{C}_{\text{GDGTs}}$). At all sites, $\delta^{13}\text{C}_{\text{BDGTs}}$ was more depleted than $\delta^{13}\text{C}_{\text{GDGTs}}$. Both Black Sea (GeoB15105) and Rhone delta (GeoB17306) sites showed very negative $\delta^{13}\text{C}_{\text{BDGTs}}$ values of $-56 \pm 1\text{‰}$ and $-41 \pm 1\text{‰}$ while the $\delta^{13}\text{C}_{\text{BDGTs}}$ were around $-28 \pm 0.1\text{‰}$ in the sapropel layers of the eastern Mediterranean basin (Fig. 5). Bp-0 from both BDGTs and GDGTs were more enriched in ^{13}C than CH_4 in each sample. On the contrary, they were more depleted in ^{13}C relative to DIC. In addition, $\delta^{13}\text{C}_{\text{GDGTs}}$ values were generally similar to $\delta^{13}\text{C}_{\text{TOC}}$, while $\delta^{13}\text{C}_{\text{BDGTs}}$ values were more negative (Fig. 5).

4 Discussion

4.1 Potential source organisms of BDGTs and PDGTs

$\delta^{13}\text{C}$ analysis of membrane lipids in environmental samples provides insight into the carbon metabolism that promoted their biosynthesis and can thus help to assign their source organisms (Hayes, 2001; Pearson, 2010). In this study, six marine sediment samples exhibiting relatively high concentrations of BDGTs and representing contrasting geochemical settings were selected for $\delta^{13}\text{C}$ analysis of lipid biomarker and carbon substrate pools to investigate the potential drivers of BDGT distributions in the environment. PDGT concentrations were too low to be analyzed for their carbon isotopic composition. BDGT-derived biphytanes ($\delta^{13}\text{C}_{\text{BDGTs}}$) exhibited systematically more negative $\delta^{13}\text{C}$ values than GDGT-derived biphytanes ($\delta^{13}\text{C}_{\text{GDGTs}}$) at all sites, pointing to a distinct origin of BDGTs (Fig. 5). Moreover, the range of $\delta^{13}\text{C}_{\text{BDGTs}}$ (between -56 and -28‰) is suggestive of a predominant benthic rather than planktonic source for these compounds (Hoefs et al., 1997; Pearson et al., 2001). Accordingly, IPL-BDGTs and IPL-PDGTs, supposedly representative of extant organisms, constituted more than 50% of the whole BDGT and PDGT pool in more than 90% of the sediment samples where they were detected (Fig. 3 and Suppl. Table 2), further supporting a benthic origin of BDGTs and PDGTs.

In the Black Sea and Rhone delta (GeoB15105 and GeoB17306), BDGT-derived biphytanes had similarly low $\delta^{13}\text{C}$ values (i.e., $< -40\text{‰}$), suggesting that BDGTs were derived from functionally related archaeal phyla at these two sites (Fig. 5). These values are also consistent with those observed by Meador et al. (2015) for IPL-BDGTs in the White Oak River Estuary, further suggesting a common source for BDGTs in these settings influenced by high inputs of terrestrial organic matter. By contrast, $\delta^{13}\text{C}_{\text{BDGTs}}$ values in the sapropel layers of the Eastern Mediterranean Basin (GeoB15103) were up to 20‰ higher than $\delta^{13}\text{C}_{\text{BDGTs}}$ values in the sediments of the Rhone delta and Black Sea (Fig. 5).

A predominant methanotrophic origin for BDGTs is unlikely, as $\delta^{13}\text{C}_{\text{BDGTs}}$ values were generally higher than $\delta^{13}\text{C}_{\text{CH}_4}$ (Fig. 5), which contrasts the relationship found in lipids from anaerobic methane-oxidizing archaea at seeps (Hinrichs et al., 1999; 2000). A methanotrophic origin for BDGTs is not likely, as $\delta^{13}\text{C}_{\text{BDGTs}}$ values were always higher than $\delta^{13}\text{C}_{\text{CH}_4}$ (Fig. 5), opposite to the relationship found in lipids from anaerobic methane-oxidizing archaea at seeps (Hinrichs et al., 1999; 2000). Pearson et al. (2010) reported fractionation effects (ϵ) between 7‰ and 36‰ between CO_2 and the produced biomass in case of autotrophic pathways. In this study, $\Delta\delta^{13}\text{C}$ between CO_2 and BDGTs was calculated considering a fractionation of -10.7‰ between dissolved CO_2 and DIC in marine sediments (Mook et al., 1974; Fig. 5). In the Rhone delta and shallow Black Sea, $\Delta\delta^{13}\text{C}$ ranged between 21‰ and 45‰ in agreement with an autotrophic metabolism consistent with the initial suggestions by Meador et al. (2015). Alternatively, it cannot be excluded that the low $\delta^{13}\text{C}_{\text{BDGTs}}$ may be due to consumption of organic substrates that are more depleted in ^{13}C than bulk TOC. In addition, some methanogenic processes, based on CO_2 fixation (hydrogenotrophic methanogenesis) or incorporation of methylated compounds (methylotrophic methanogenesis), induce large carbon isotopic fractionation during lipid biosynthesis (Londry et al., 2008; Summons et al., 1998) and could also explain the relatively low $\delta^{13}\text{C}_{\text{BDGTs}}$ values (i.e. $< -20\text{‰}$). On the contrary, in the sapropels and in the deeper horizon of the Black Sea,

$\Delta\delta^{13}\text{C}_{\text{CO}_2\text{-BDGT}}$ ranged between 9‰ and 12‰ (Fig. 5). This suggests an alternative carbon metabolism and/or phylogenetic group of BDGT producers. In particular, the heterotrophic incorporation of organic compounds usually induces a small isotopic fractionation between the substrates and the membrane lipids (Pearson, 2010). Some methanogens can use acetate as a carbon source and a small isotopic fractionation has been observed in this case (Londry et al., 2008; Summons et al., 1998). This could hold true for the deep sample from the Black Sea. However, the relatively high concentrations of BDGTs and PDGTs in the Mediterranean sapropel samples (Suppl. Table 2) combined with low rates of methanogenesis, as indicated by the low CH_4 concentrations (Suppl. Table 1), strongly suggest that methanogens cannot account for the BDGT pool in this setting. It is therefore likely that other archaea with non-methanogenic metabolisms are the sources of BDGTs in the Mediterranean sapropels.

Multivariate analysis of the marine sediment sample set ($n = 48$; Fig. 4) distinguished three BDGT and PDGT distribution patterns. The eastern Mediterranean Basin samples clustered with the other basin site samples of the dataset (Marmara Sea, Cap de Creus and Ligurian-Provençal Basin; Fig. 4). The Black Sea samples formed a second cluster and the Rhone delta samples formed the last cluster in the PCA. The first two clusters were characterized by a predominance of 1G-BDGTs (and 1G-PDGTs; Suppl. Table 2) but the Black Sea differed from the other basin sites due to higher proportions of CL-BDGTs than in the rest of the sample set ~~and as well as the~~ absence of PDGTs. Additional contribution of BDGTs produced within the anoxic Black Sea bottom waters (Schröder, 2015) could explain the higher proportion of CL-BDGTs at this site. On the contrary, the last cluster (formed by Rhone delta samples) showed a predominance of 2G-BDGTs and 2G-PDGTs (Fig. 4). Meador et al. (2015) similarly observed a higher relative abundance of 2G-BDGTs and 2G-PDGTs in the White Oak River Estuary, another river mouth highly influenced by terrestrial input. By contrast, only 1G bearing BDGTs were observed in the membrane of *M. luminyensis* (Becker et al., 2016). This contrasted distribution pattern argues for a distinct, estuarine-based, archaeal community producing BDGTs.

Overall, our data infer that BDGT (and PDGT) producers may comprise an autotrophic, potentially methanogenic community as well as a heterotrophic, likely not methanogenic community. A methanogenic origin of BDGTs (and PDGTs) is in agreement with their prominence in *M. luminyensis* (Becker et al., 2016), the only cultured representative of Methanomassiliicoccales, a novel order of methanogens (Dridi et al., 2012). However, heterotrophic (acetate) C incorporation was so far suggested for Methanomassiliicoccales (Borrel et al., 2014; Lang et al., 2015; Söllinger et al., 2016), which cannot explain the observed carbon isotopic composition of BDGTs in the Rhone delta and the Black Sea if we consider the $\delta^{13}\text{C}$ of acetate to be similar to $\delta^{13}\text{C}_{\text{TOC}}$. More studies on Methanomassiliicoccales carbon metabolism are needed to accurately relate the presence of BDGTs in the environment to this archaeal group. Furthermore, the similar distributions of BDGTs and 16S rRNA gene clones from Bathyarchaeota in estuarine sediments led Meador et al. (2015) to suggest that this group is a putative source of BDGTs. Bathyarchaeota are widespread in marine sediments, notably in the deep subsurface horizons (e.g. Lloyd et al., 2013). They are phylogenetically highly diverse (e.g. Lazar et al., 2015) and contain diverse metabolic groups (e.g. Lazar et al., 2016; Yu et al., 2018; Zhou et al., 2018) involving both autotrophic and heterotrophic lifestyles. Methanogenic capacities have also been identified for some members of this clade (Evans et al., 2015). The contrasted BDGT carbon isotopic composition observed in the different sites of the present study could thus be explained by these versatile metabolic capabilities. It is thus conceivable that the ubiquitous Bathyarchaeota, including methanogens, are an additional source for BDGTs (and PDGTs) in the environment.

4.2 BDGTs as a putative adaptive trait of subsurface archaea

Zhu et al. (2014) demonstrated the 1,2,3 butanetriol structure of the BDGT backbone via gas chromatography MS, following ether cleavage from its biphytanyl chains. In the present study, 2D-NMR analysis confirmed the presence of a butanetriol backbone and unequivocally determined its configuration in the tetraether molecule (Fig. 2). Additional methylations have been previously observed on the ~~side-isoprenoid~~ chains or as methoxylation on the glycerol in different lipid classes (e.g. Elling

et al., 2017; Knappy et al., 2015). However, BDGTs (and PDGTs) stand out as unique archaeal membrane lipids that contain a non-glycerol moiety. This raises two fundamental questions: (i) how are these lipids biosynthesized? and (ii) why do microorganisms produce them?

For every domain of life, it is known that dihydroxyacetone phosphate (DHAP), an intermediate in glycolysis, serves as a precursor of the glycerol moiety in membrane lipid backbones (Koga and Morii, 2007). At the early stage of membrane lipid biosynthesis, DHAP is converted by stereospecific glycerol dehydrogenase enzymes into either a glycerol-3-phosphate (G-3-P) or a glycerol-1-phosphate (G-1-P) in Bacteria and Archaea, respectively. The existence of BDGTs (and PDGTs) imply that different precursors must be involved at the very first steps of lipid biosynthesis. Knappy et al. (2014) suggested, for example, the involvement of putative butanetriol or pentanetriol phosphate. However, in the genomes of Methanomassiliicoccales, only one gene for 3-O-geranylgeranyl-sn-glyceryl-1-phosphate (GGGP) synthase was identified (Becker et al., 2016), but no second homologue that might encode a hypothetical enzyme catalyzing the formation of butanetriol- or pentanetriol-based intermediates. Alternatively, BDGTs and PDGTs could be regular GDGTs, which underwent additional methylation at the final stages of their biosynthesis. Welander et al. (2010) showed that an S-adenosylmethionine (SAM) enzyme catalyzing a radical reaction was responsible for the methylation of certain bacterial hopanoids at the C2 position. We found 13 genes annotated as belonging to the radical SAM superfamily in the permanent draft genome of *M. luminyensis* B10 (IMG/M website, IMG Submission ID 11458; Chen et al., 2019). Very recently, another SAM enzyme was proposed to be involved in the biosynthesis of calditol based lipids in the archaeal strain *Sulfolobus acidocaldarius* (Zeng et al., 2018). A similar mechanism could explain the structure of BDGTs and PDGTs. The recent observation of such radical-mediated reactions on un-activated carbon atoms in both bacterial and archaeal strains (Zhou et al., 2016) implies that this may be a common mechanism to adapt their lipid envelope to the surrounding environment.

The ubiquitous presence of BDGTs and PDGTs in the environment and their active biosynthesis by certain organisms, notably *M. luminyensis* (Becker et al., 2016), signify that they have likely offered an evolutionary advantage to their producers. Two trends emerged from the concentration and distribution of BDGTs and PDGTs in the Mediterranean and the Black Seas. First, the proportion of BDGTs and PDGTs relative to GDGT-0 ((sum-BDGTs)/(sum-GDGT-0), (sum-PDGTs)/(sum-GDGT-0)) remained stable or even increased with depth (Suppl. Table 2). Moreover, unlike GDGT-0, the IPL form of BDGTs and PDGTs dominates their distribution at every depth (Fig. 3). This suggests that IPL-BDGTs and IPL-PDGTs may be specifically produced by sedimentary archaea, as Meador et al. (2015) previously proposed, and/or that they are more resistant against extracellular hydrolytic enzymes. The highest constraint for life in subsurface sediments is the lack of energy, which selects for microorganisms that limit their energy requirement to the most essential functions (e.g. Bradley et al., 2019; Hoehler and Jørgensen, 2013). Hypothetically, the additional methyl or ethyl group could increase the stability of the cell membrane by sterically hindering access of extracellular enzymes and responsible for the thereby-lysis of the glycosidic bond that links the mono- or disaccharide headgroups, thereby preserving the IPL form and decreasing the maintenance energy demand of these organisms for lipid repair.

5 Conclusion

The unique structure of BDGTs, here unambiguously elucidated by NMR experiments, further increases the diversity of membrane lipids observed in Archaea. BDGTs and PDGTs were detected in a large set of marine sediment samples from diverse geochemical, depth and age conditions, highlighting their widespread presence in marine sediments. ~~The concentration and distribution of BDGTs and PDGTs as well as the stable C isotopic signature of BDGTs contrast with the observed trends for GDGT-0 suggesting a distinct role in the cell membranes.~~ Within the dataset, major differences are also observed in the BDGT and PDGT headgroup distribution patterns and ^{13/12}C content of BDGT-derived biphytanes relative to DIC. ~~Thus, it~~ seems ~~thus~~ likely that BDGT and PDGT biosynthesis may be present across different archaeal phyla relying on different carbon

metabolisms. A common trait of the subseafloor sample set is the high contribution of BDGTs, especially in their intact polar form, to the total lipid pool. The specific 1,2,3 butanetriol structure of their backbone could then be interpreted as an adaptive trait of sedimentary archaea to energy limited environments.

Data availability

365 Data will be made available in PANGAEA under <https://doi.org/10.1594/PANGAEA.###>.

Sample availability

Samples are stored at MARUM – Center for Marine Environmental Sciences, University of Bremen, Germany. Sample aliquots may be requested from Prof. Dr. Kai-Uwe Hinrichs.

Appendices

370 Supplementary Table 1: Sample general properties, organic matter and geochemical parameters.

Supplementary Table 2: Absolute concentration, relative abundance and distribution indices of GDGTs, BDGTs and PDGTs.

Supplementary Table 3: Carbon isotopic composition ($\delta^{13}\text{C}$) of the biphytanes derived from IPL-GDGT-0 and IPL-BDGT-0 together with the carbon isotopic composition of the total organic carbon (TOC), dissolved inorganic carbon (DIC) and methane.

375 [Supplementary Figure 1: 1D \$^1\text{H}\$ spectrum and expansions of BDGT-0 in \$\text{CDCl}_3\$.](#)

[Supplementary Figure 2: \$^1\text{H}\$ - \$^{13}\text{C}\$ HSQC two-dimensional spectra of BDGT-0.](#)

[Supplementary Figure 3: \$^1\text{H}\$ - \$^{13}\text{C}\$ HMBC two-dimensional spectra of BDGT-0.](#)

Author contribution

380 S.C., K.-U.H., J.S.L. and V.B.H. designed the study; S.C., T.B.M., K.W.B. and J.S. performed laboratory work and lipid quantification; L.M. and Q.-Z.Z. performed the isotope analysis; M.P.C. performed the NMR-based structural elucidation; V.B.H. selected sites and led sample collection and curation; S.C. performed the statistical analysis, interpreted the results and wrote the paper with significant input from T.B.M. and K.U.H.; all co-authors commented on the manuscript.

Competing interests

The authors declare that they have no conflict of interest.

385

Acknowledgements

390 The authors acknowledge the participants and the crew members of the two DARCSEAS cruises: RV *Meteor* Cruise M84/1 and RV *Poseidon* Cruise POS450. Jenny Wendt and Jessica Arndt are thanked for their help in the laboratory and for providing the CH_4 and DIC carbon isotopic compositions. [We also thank the associate editor Dr. Marcel van der Meer, Dr. Darci Rush and an anonymous reviewer for their constructive comments that helped improve this manuscript.](#) This study was funded by the European Research Council under the European Union's Seventh Framework Program – “Ideas” Specific Program, ERC grant agreement #247153 (Advanced Grant DARCLIFE; P.I. K.-U.H), the Deutsche Forschungsgemeinschaft through the Gottfried-Wilhelm Leibniz Program (Award HI 616-14-1) and by the University of Bremen through its excellence program

“M8 Post-Doc Initiative” awarded to S.C. T.B.M. was additionally supported by MEYS CZ grant LM2015075 Projects of Large Infrastructure for Research, Development and Innovations as well as the European Regional Development Fund-Project: research of key soil-water ecosystem interactions at the SoWa Research Infrastructure (No. CZ.02.1.01/0.0/0.0/16_013/0001782).

References

- Becker, K.W., Elling, F.J., Yoshinaga, M.Y., Söllinger, A., Urich, T., Hinrichs, K.-U.: Unusual butane- and pentanetriol-based tetraether lipids in *Methanomassiliicoccus luminyensis*, a representative of the seventh order of methanogens, Appl. Environ. Microbiol. **82**, 4505–4516, AEM.00772-16, <https://doi.org/10.1128/AEM.00772-16>, 2016.
- Becker, K.W., Lipp, J.S., Versteegh, G.J.M., Wörmer, L., Hinrichs, K.-U.: Rapid and simultaneous analysis of three molecular sea surface temperature proxies and application to sediments from the Sea of Marmara, Org. Geochem. **85**, 42–53, <https://doi.org/10.1016/j.orggeochem.2015.04.008>, 2015.
- Biddle, J.F., Lipp, J.S., Lever, M.A., Lloyd, K.G., Sørensen, K.B., Anderson, R., Fredricks, H.F., Elvert, M., Kelly, T.J., Schrag, D.P., Sogin, M.L., Brenchley, J.E., Teske, A., House, C.H., Hinrichs, K.-U.: Heterotrophic Archaea dominate sedimentary subsurface ecosystems off Peru, Proc. Natl. Acad. Sci. **103**, 3846–3851, <https://doi.org/10.1073/pnas.0600035103>, 2006.
- Borrel, G., Parisot, N., Harris, H.M., Peyretailade, E., Gaci, N., Tottey, W., Bardot, O., Raymann, K., Gribaldo, S., Peyret, P., O’Toole, P.W., Brugère, J.-F.: Comparative genomics highlights the unique biology of Methanomassiliicoccales, a Thermoplasmatales-related seventh order of methanogenic archaea that encodes pyrrolysine, BMC Genomics **15**, 679, <https://doi.org/10.1186/1471-2164-15-679>, 2014.
- Bradley, J.A., Amend, J.P., LaRowe, D.E.: Survival of the fewest: Microbial dormancy and maintenance in marine sediments through deep time, Geobiology **17**, 43–59, <https://doi.org/10.1111/gbi.12313>, 2019.
- Chen, I.-M.A., Chu, K., Palaniappan, K., Pillay, M., Ratner, A., Huang, J., Huntemann, M., Varghese, N., White, J.R., Seshadri, R., Smirnova, T., Kirton, E., Jungbluth, S.P., Woyke, T., Eloë-Fadrosch, E.A., Ivanova, N.N., Kyrpides, N.C.: IMG/M v.5.0: an integrated data management and comparative analysis system for microbial genomes and microbiomes, Nucleic Acids Res. **47**, D666–D677, <https://doi.org/10.1093/nar/gky901>, 2019.
- De Rosa, M., Gambacorta, A.: The Lipids of Archaeobacteria, Prog. Lipid Res. **27**, 153–175, [https://doi.org/10.1016/0163-7827\(88\)90011-2](https://doi.org/10.1016/0163-7827(88)90011-2), 1988.
- Dridi, B., Fardeau, M.-L., Ollivier, B., Raoult, D., Drancourt, M.: *Methanomassiliicoccus luminyensis* gen. nov., sp. nov., a methanogenic archaeon isolated from human faeces, Int. J. Syst. Evol. Microbiol. **62**, 1902–1907, <https://doi.org/10.1099/ijs.0.033712-0>, 2012.
- Elling, F.J., Könneke, M., Lipp, J.S., Becker, K.W., Gagen, E.J., Hinrichs, K.-U.: Effects of growth phase on the membrane lipid composition of the thaumarchaeon *Nitrosopumilus maritimus* and their implications for archaeal lipid distributions in the marine environment, Geochim. Cosmochim. Acta. **141**, 579–597, <https://doi.org/10.1016/j.gca.2014.07.005>, 2014.
- Elling, F.J., Könneke, M., Nicol, G.W., Stieglmeier, M., Bayer, B., Spieck, E., Torre, J.R. de la, Becker, K.W., Thomm, M., Prosser, J.I., Herndl, G.J., Schleper, C., Hinrichs, K.-U.: Chemotaxonomic characterisation of the thaumarchaeal lipidome, Environ. Microbiol. **19**, 2681–2700, <https://doi.org/10.1111/1462-2920.13759>, 2017.
- Evans, P.N., Parks, D.H., Chadwick, G.L., Robbins, S.J., Orphan, V.J., Golding, S.D., Tyson, G.W.: Methane metabolism in the archaeal phylum Bathyarchaeota revealed by genome-centric metagenomics, Science **350**, 434–438, <https://doi.org/10.1126/science.aac7745>, 2015.
- Hayes, J.M.: Fractionation of Carbon and Hydrogen Isotopes in Biosynthetic Processes, Rev. Mineral. Geochem. **43**, 225–277, <https://doi.org/10.2138/gsrmg.43.1.225>, 2001.

- 435 Heuer, V.B., Aiello, I.W., Elvert, M., Goldenstein, N.I., Goldhammer, T., Könneke, M., Liu, X., Pape, T., Schmidt, F., Wendt, J., Zhuang, G.: Report and preliminary results of R/V POSEIDON cruise POS450, DARCSEAS II – Deep seafloor Archaea in the Western Mediterranean Sea: Carbon Cycle, Life Strategies, and Role in Sedimentary Ecosystems, Barcelona (Spain) – Malaga (Spain), April 2 – 13, 2013 (No. 305), Berichte, MARUM – Zentrum für Marine Umweltwissenschaften, Fachbereich Geowissenschaften, Universität Bremen, Bremen, 2014.
- 440 Hinrichs, K.-U., Hayes, J.M., Sylva, S.P., Brewer, P.G., DeLong, E.F.: Methane-consuming archaeobacteria in marine sediments *Nature* 398, 802–805, <https://doi.org/10.1038/19751>, 1999.
- Hinrichs, K.-U., Summons, R.E., Orphan, V., Sylva, S.P., Hayes, J.M.: Molecular and isotopic analysis of anaerobic methane-oxidizing communities in marine sediments, *Org. Geochem.* 31, 1685–1701, [https://doi.org/10.1016/S0146-6380\(00\)00106-6](https://doi.org/10.1016/S0146-6380(00)00106-6), 2000.
- 445 Hoefs, M.J.L., Schouten, S., Leeuw, J.W.D., King, L.L., Wakeham, S.G., Damsté, J.S.S.: Ether Lipids of Planktonic Archaea in the Marine Water Column, *Appl. Env. Microbiol.* 63, 63090–3095, 1997.
- Hoehler, T.M., Jørgensen, B.B.: Microbial life under extreme energy limitation, *Nat. Rev. Microbiol.* 11, 83–94, <https://doi.org/10.1038/nrmicro2939>, 2013.
- Kates, M.: The phytanyl ether-linked polar lipids and isoprenoid neutral lipids of extremely halophilic bacteria, *Prog. Chem. Fats Other Lipids* 15, 301–342, [https://doi.org/10.1016/0079-6832\(77\)90011-8](https://doi.org/10.1016/0079-6832(77)90011-8), 1977.
- 450 Kellermann, M.Y., Wegener, G., Elvert, M., Yoshinaga, M.Y., Lin, Y.-S., Holler, T., Mollar, X.P., Knittel, K., Hinrichs, K.-U.: Autotrophy as a predominant mode of carbon fixation in anaerobic methane-oxidizing microbial communities, *Proc. Natl. Acad. Sci.* 109, 19321–19326, <https://doi.org/10.1073/pnas.1208795109>, 2012.
- Knappy, C., Barillà, D., Chong, J., Hodgson, D., Morgan, H., Suleman, M., Tan, C., Yao, P., Keely, B.: Mono-, di- and trimethylated homologues of isoprenoid tetraether lipid cores in archaea and environmental samples: mass spectrometric identification and significance, *J. Mass Spectrom.* 50, 1420–1432, <https://doi.org/10.1002/jms.3709>, 2015.
- 455 Knappy, C.S., Yao, P., Pickering, M.D., Keely, B.J.: Identification of homoglycerol- and dihomoglycerol-containing isoprenoid tetraether lipid cores in aquatic sediments and a soil, *Org. Geochem.* 76, 146–156, <https://doi.org/10.1016/j.orggeochem.2014.06.003>, 2014.
- 460 Koga, Y., Morii, H.: Recent Advances in Structural Research on Ether Lipids from Archaea Including Comparative and Physiological Aspects, *Biosci. Biotechnol. Biochem.* 69, 2019–2034, <https://doi.org/10.1271/bbb.69.2019>, 2005.
- Koga, Y., Morii, H.: Biosynthesis of Ether-Type Polar Lipids in Archaea and Evolutionary Considerations, *Microbiol. Mol. Biol. Rev.* 71, 97–120, <https://doi.org/10.1128/MMBR.00033-06>, 2007.
- Koga, Y., Nishihara, M., Morii, H., Akagawa-Matsushita, M.: Ether polar lipids of methanogenic bacteria: structures, comparative aspects, and biosynthesis, *Microbiol. Rev.* 57, 164–182, 1993.
- 465 Lang, K., Schuldes, J., Klingl, A., Poehlein, A., Daniel, R., Brune, A.: New Mode of Energy Metabolism in the Seventh Order of Methanogens as Revealed by Comparative Genome Analysis of “*Candidatus Methanoplasma termitum*”, *Appl. Environ. Microbiol.* 81, 1338–1352, <https://doi.org/10.1128/AEM.03389-14>, 2015.
- Lazar, C.S., Baker, B.J., Seitz, K., Hyde, A.S., Dick, G.J., Hinrichs, K.-U., Teske, A.P.: Genomic evidence for distinct carbon substrate preferences and ecological niches of Bathyarchaeota in estuarine sediments, *Environ. Microbiol.* 18, 1200–1211, <https://doi.org/10.1111/1462-2920.13142>, 2016.
- 470 Lazar, C.S., Biddle, J.F., Meador, T.B., Blair, N., Hinrichs, K.-U., Teske, A.P.: Environmental controls on intragroup diversity of the uncultured benthic archaea of the miscellaneous Crenarchaeotal group lineage naturally enriched in anoxic sediments of the White Oak River estuary (North Carolina, USA), *Environ. Microbiol.* 17, 2228–2238, <https://doi.org/10.1111/1462-2920.12659>, 2015.

- Liu, X.-L., Summons, R.E., Hinrichs, K.-U.: Extending the known range of glycerol ether lipids in the environment: structural assignments based on tandem mass spectral fragmentation patterns, *Rapid Commun. Mass Spectrom.* 26, 2295–2302, <https://doi.org/10.1002/rcm.6355>, 2012.
- Lloyd, K.G., Schreiber, L., Petersen, D.G., Kjeldsen, K.U., Lever, M.A., Steen, A.D., Stepanauskas, R., Richter, M., Kleindienst, S., Lenk, S., Schramm, A., Jørgensen, B.B.: Predominant archaea in marine sediments degrade detrital proteins, *Nature* 496, 215–218, <https://doi.org/10.1038/nature12033>, 2013.
- Lombard, J., López-García, P., Moreira, D.: The early evolution of lipid membranes and the three domains of life, *Nat. Rev. Microbiol.* 10, 507–515, <https://doi.org/10.1038/nrmicro2815>, 2012.
- Londry, K.L., Dawson, K.G., Grover, H.D., Summons, R.E., Bradley, A.S.: Stable carbon isotope fractionation between substrates and products of *Methanosarcina barkeri*, *Org. Geochem.* 39, 608–621, <https://doi.org/10.1016/j.orggeochem.2008.03.002>, 2008.
- Meador, T.B., Bowles, M., Lazar, C.S., Zhu, C., Teske, A., Hinrichs, K.-U: The archaeal lipidome in estuarine sediment dominated by members of the Miscellaneous Crenarchaeotal Group: Archaeal lipid distributions in the WOR estuary, *Environ. Microbiol.* 17, 2441–2458, <https://doi.org/10.1111/1462-2920.12716>, 2015.
- Meador, T.B., Gagen, E.J., Loscar, M.E., Goldhammer, T., Yoshinaga, M.Y., Wendt, J., Thomm, M., Hinrichs, K.-U.: *Thermococcus kodakarensis* modulates its polar membrane lipids and elemental composition according to growth stage and phosphate availability, *Front. Microbiol.* 5, <https://doi.org/10.3389/fmicb.2014.00010>, 2014.
- Mook, W.G., Bommerson, J.C., Staverman, W.H.: Carbon isotope fractionation between dissolved bicarbonate and gaseous carbon dioxide, *Earth Planet. Sc. Lett.* 22, 169–176, [https://doi.org/10.1016/0012-821X\(74\)90078-8](https://doi.org/10.1016/0012-821X(74)90078-8), 1974.
- Pancost, R.D., Bouloubassi, I., Aloisi, G., Sinninghe Damsté, J.S., Scientific Party, the M.S.: Three series of non-isoprenoidal dialkyl glycerol diethers in cold-seep carbonate crusts, *Org. Geochem.* 32, 695–707, [https://doi.org/10.1016/S0146-6380\(01\)00015-8](https://doi.org/10.1016/S0146-6380(01)00015-8), 2001.
- Paściak, M., Holst, O., Lindner, B., Mordarska, H., Gamian, A.: Novel Bacterial Polar Lipids Containing Ether-linked Alkyl Chains, the Structures and Biological Properties of the Four Major Glycolipids from *Propionibacterium propionicum* PCM 2431 (ATCC 14157 T), *J. Biol. Chem.* 278, 3948–3956, <https://doi.org/10.1074/jbc.M206013200>, 2003.
- Pearson, A.: Pathways of Carbon Assimilation and Their Impact on Organic Matter Values $\delta^{13}\text{C}$, in: *Handbook of Hydrocarbon and Lipid Microbiology*, Springer, Berlin, Heidelberg, 143–156, https://doi.org/10.1007/978-3-540-77587-4_9, 2010.
- Pearson, A., ~~Menichet~~ McNichol, A.P., Benitez-Nelson, B.C., Hayes, J.M., Eglinton, T.I.: Origins of lipid biomarkers in Santa Monica Basin surface sediment: A case study using compound-specific $\Delta^{14}\text{C}$ analysis, *Geochim. Cosmochim. Acta* 65, [453123–3137](https://doi.org/10.1016/S0016-7169(01)00313-3), 2001.
- Pitcher, A., Hopmans, E.C., Schouten, S., Sinninghe Damsté, J.S.: Separation of core and intact polar archaeal tetraether lipids using silica columns: Insights into living and fossil biomass contributions. *Organic Geochemistry* 40, 12–19. <https://doi.org/10.1016/j.orggeochem.2008.09.008>, 2009.
- Reeburgh, W.S.: Oceanic Methane Biogeochemistry. *Chem. Rev.* 107, 486–513. <https://doi.org/10.1021/cr050362v>, 2007.
- Rütters, H., Sass, H., Cypionka, H., Rullkötter, J.: Monoalkylether phospholipids in the sulfate-reducing bacteria *Desulfosarcina variabilis* and *Desulforhabdus amnigenus*, *Arch. Microbiol.* 176, 435–442, <https://doi.org/10.1007/s002030100343>, 2001.
- Schmidt, F., Koch, B.P., Goldhammer, T., Elvert, M., Witt, M., Lin, Y.-S., Wendt, J., Zabel, M., Heuer, V.B., Hinrichs, K.-U.: Unraveling signatures of biogeochemical processes and the depositional setting in the molecular composition of pore water DOM across different marine environments, *Geochim. Cosmochim. Acta* 207, 57–80, <https://doi.org/10.1016/j.gca.2017.03.005>, 2017.

- Schouten, S., Hopmans, E.C., Pancost, R.D., Damsté, J.S.S.: Widespread occurrence of structurally diverse tetraether membrane lipids: Evidence for the ubiquitous presence of low-temperature relatives of hyperthermophiles, *Proc. Natl. Acad. Sci.* 97, 14421–14426, <https://doi.org/10.1073/pnas.97.26.14421>, 2000.
- Schouten, S., Hopmans, E.C., Sinninghe Damsté, J.S.: The organic geochemistry of glycerol dialkyl glycerol tetraether lipids: A review, *Org. Geochem.* 54, 19–61, <https://doi.org/10.1016/j.orggeochem.2012.09.006>, 2013.
- Schubotz, F., Lipp, J.S., Elvert, M., Hinrichs, K.-U.: Stable carbon isotopic compositions of intact polar lipids reveal complex carbon flow patterns among hydrocarbon degrading microbial communities at the Chapopote asphalt volcano, *Geochim. Cosmochim. Acta* 75, 4399–4415, <https://doi.org/10.1016/j.gca.2011.05.018>, 2011.
- Schröder, J.M., Intact polar lipids in marine sediments: improving analytical protocols and assessing planktonic and benthic sources. PhD thesis, Universität Bremen, Bremen, Germany, 2015.
- Sinninghe Damsté, J.S., Schouten, S., Hopmans, E.C., Duin, A.C.T. van, Geenevasen, J.A.J.: Crenarchaeol the characteristic core glycerol dibiphytanyl glycerol tetraether membrane lipid of cosmopolitan pelagic crenarchaeota, *J. Lipid Res.* 43, 1641–1651, <https://doi.org/10.1194/jlr.M200148-JLR200>, 2002.
- Söllinger, A., Schwab, C., Weinmaier, T., Loy, A., Tveit, A.T., Schleper, C., Urich, T.: Phylogenetic and genomic analysis of *Methanomassiliicoccales* in wetlands and animal intestinal tracts reveals clade-specific habitat preferences, *FEMS Microbiol. Ecol.* 92, fiv149, <https://doi.org/10.1093/femsec/fiv149>, 2016.
- Sturt, H.F., Summons, R.E., Smith, K., Elvert, M., Hinrichs, K.-U.: Intact polar membrane lipids in prokaryotes and sediments deciphered by high-performance liquid chromatography/electrospray ionization multistage mass spectrometry—new biomarkers for biogeochemistry and microbial ecology, *Rapid Commun. Mass Spectrom.* 18, 617–628, <https://doi.org/10.1002/rcm.1378>, 2004.
- Summons, R.E., Franzmann, P.D., Nichols, P.D.: Carbon isotopic fractionation associated with methylotrophic methanogenesis, *Org. Geochem.* 28, 465–475, [https://doi.org/10.1016/S0146-6380\(98\)00011-4](https://doi.org/10.1016/S0146-6380(98)00011-4), 1998.
- Vinçon-Laugier, A., Grossi, V., Pacton, M., Escarguel, G., Cravo-Laureau, C.: The alkyl glycerol ether lipid composition of heterotrophic sulfate reducing bacteria strongly depends on growth substrate, *Org. Geochem.* 98, 141–154, <https://doi.org/10.1016/j.orggeochem.2016.05.015>, 2016.
- Weijers, J.W.H., Schouten, S., Hopmans, E.C., Geenevasen, J.A.J., David, O.R.P., Coleman, J.M., Pancost, R.D., Sinninghe Damsté, J.S.: Membrane lipids of mesophilic anaerobic bacteria thriving in peats have typical archaeal traits, *Environ. Microbiol.* 8, 648–657, <https://doi.org/10.1111/j.1462-2920.2005.00941.x>, 2006.
- Welander, P.V., Coleman, M.L., Sessions, A.L., Summons, R.E., Newman, D.K.: Identification of a methylase required for 2-methylhopanoid production and implications for the interpretation of sedimentary hopanes, *Proc. Natl. Acad. Sci.* 107, 8537–8542, <https://doi.org/10.1073/pnas.0912949107>, 2010.
- Wessel, P., Smith, W.H.F., Scharroo, R., Luis, J., Wobbe, F.: Generic Mapping Tools: Improved Version Released, *Eos* 94, 409–410, <https://doi.org/10.1002/2013EO450001>, 2013.
- Woese, C.R., Kandler, O., Wheelis, M.L.: Towards a Natural System of Organisms: Proposal for the Domains Archaea, Bacteria, and Eucarya, *Proc. Natl. Acad. Sci. U. S. A.* 87, 4576–4579, 1990.
- Yu, T., Wu, W., Liang, W., Lever, M.A., Hinrichs, K.-U., Wang, F.: Growth of sedimentary Bathyarchaeota on lignin as an energy source, *Proc. Natl. Acad. Sci.* 115, 6022–6027, <https://doi.org/10.1073/pnas.1718854115>, 2018.
- Zabel, M.: RV METEOR, Cruise Report M84/L1, Biogeochemistry and methane hydrates of the Black Sea; Oceanography of the Mediterranean; Shelf sedimentation and cold water carbonates. DFG Senatskommission für Ozeanographie c/o MARUM – Zentrum für Marine Umweltwissenschaften, Bremen, 2011.
- Zeng, Z., Liu, X.-L., Wei, J.H., Summons, R.E., Welander, P.V.: Calditol-linked membrane lipids are required for acid tolerance in *Sulfolobus acidocaldarius*, *Proc. Natl. Acad. Sci.* 115, 12932–12937, <https://doi.org/10.1073/pnas.1814048115>, 2018.

- Zhou, S., Alkhalaf, L.M., de los Santos, E.L., Challis, G.L.: Mechanistic insights into class B radical-S-adenosylmethionine methylases: ubiquitous tailoring enzymes in natural product biosynthesis, *Curr. Opin. Chem. Biol.* 35, 73–79, <https://doi.org/10.1016/j.cbpa.2016.08.021>, 2016.
- 565 Zhou, Z., Pan, J., Wang, F., Gu, J.-D., Li, M.: Bathyarchaeota: globally distributed metabolic generalists in anoxic environments, *FEMS Microbiol. Rev.* 42, 639–655, <https://doi.org/10.1093/femsre/fuy023>, 2018.
- Zhu, C., Lipp, J.S., Wörmer, L., Becker, K.W., Schröder, J., Hinrichs, K.-U.: Comprehensive glycerol ether lipid fingerprints through a novel reversed phase liquid chromatography–mass spectrometry protocol, *Org. Geochem.* 65, 53–62, <https://doi.org/10.1016/j.orggeochem.2013.09.012>, 2013.
- 570 Zhu, C., Meador, T.B., Dumann, W., Hinrichs, K.-U.: Identification of unusual butanetriol dialkyl glycerol tetraether and pentanetriol dialkyl glycerol tetraether lipids in marine sediments, *Rapid Commun. Mass Spectrom.* 28, 332–338, <https://doi.org/10.1002/rcm.6792>, 2014.

Table

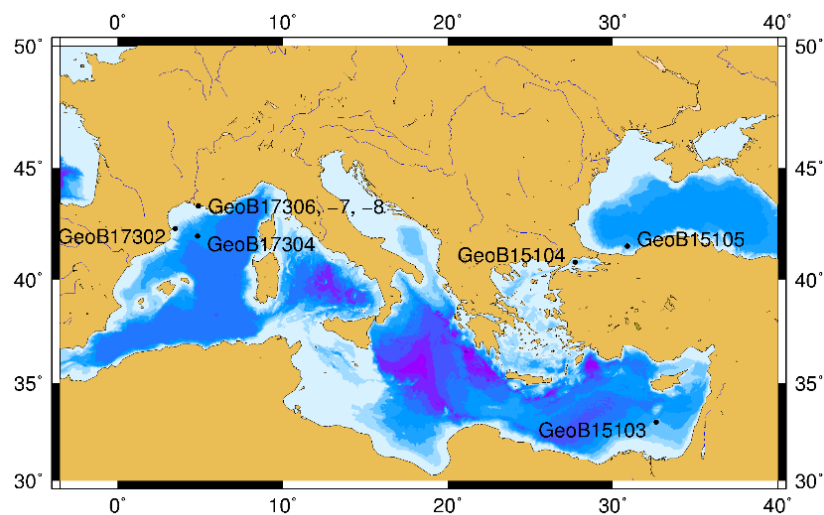
Table 1: ¹³C- and ¹H-NMR chemical shifts of BDGT-0 as well as key correlations from ¹H-¹³C HSQC and HMBC spectra.

Carbon numbers correspond to the carbon atoms in Fig. 2. Overlapped peaks are given as ranges (i.e. 1.17-1.21 ppm).

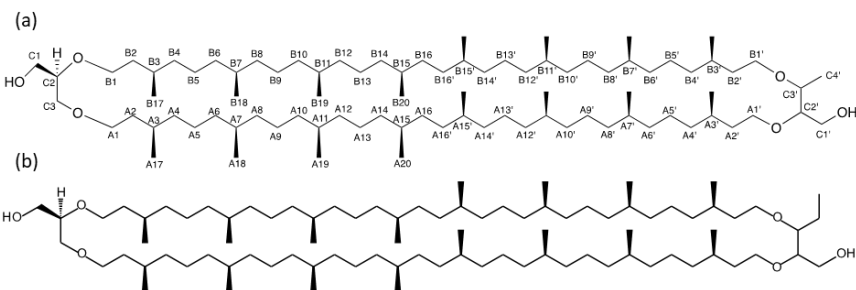
| | $\delta^{13}\text{C}$ (ppm) | | | $\delta^1\text{H}$ (ppm) | Key correlations observed in the ¹ H- ¹³ C HSQC and HMBC spectra |
|--|-----------------------------|-----------------|-------------------------------|--|--|
| Carbon number | CH ₃ | CH ₂ | CH | | |
| <u>A1</u> | | <u>70.10</u> | | <u>3.45</u> | Strong degenerate methylene signal in ¹ H- ¹³ C HSQC; HMBC correlations to A2, A3 and C3 (across ether linkage). |
| <u>A1'</u> | | <u>68.78</u> | | <u>3.56</u> | Strong degenerate methylene signal in ¹ H- ¹³ C HSQC; HMBC correlations to A2' and A3' and C2' (across ether linkage). |
| <u>B1</u> | | <u>68.56</u> | | <u>3.52 ; 3.64</u> | See B2. |
| <u>B1'</u> | | <u>67.40</u> | | <u>3.39 ; 3.58</u> <u>(dt, J = 7.0, 8.8 Hz)</u> | See B2' for correlations. Non-degenerate methylene pair. |
| <u>A2</u> | | <u>36.66</u> | | <u>1.33 ; 1.59</u> | ¹ H- ¹³ C HMBC correlations to A1. |
| <u>A2'</u> | | <u>37.03</u> | | <u>1.37 ; 1.58</u> | Signals overlapped in ¹ H- ¹³ C HSQC but resolution afforded by ¹ H- ¹³ C HMBC correlations to A1', B1 and B1'. |
| <u>B2</u> | | <u>37.03</u> | | <u>1.36 ; 1.60</u> | |
| <u>B2'</u> | | <u>37.03</u> | | <u>1.32 ; 1.57</u> | |
| <u>A3</u> | | | <u>29.71</u> | <u>1.51</u> | Signals overlapped in ¹ H- ¹³ C HSQC, single positive (methine) signal observed, but A3, A3' resolved by HMBC. B3, B3' correlations too weak to distinguish due to multiplicity of B1, B1' correlations. |
| <u>A3'</u> | | | <u>29.54</u> | <u>1.51</u> | |
| <u>B3, B3'</u> | | | <u>29.60</u> | <u>1.51</u> | |
| <u>A4, A4', B4, B4'</u> <u>A6, A6', B6, B6'</u> <u>A8, A8', B8, B8'</u> <u>A10, A10', B10, B10'</u> <u>A12, A12', B12, B12'</u> <u>A14, A14', B14, B14'</u> | | <u>37.35</u> | | <u>1.02-1.11;</u> <u>1.21-1.27</u> | |
| <u>A5, A5', B5, B5'</u> <u>A9, A9', B9, B9'</u> <u>A13, A13', B13, B13'</u> | | | <u>24.36,</u> <u>24.45</u> | <u>1.17-1.21;</u> <u>1.27-1.30</u> | |
| <u>A7, A7', B7, B7'</u> <u>A11, A11', B11, B11'</u> <u>A15, A15', B15, B15'</u> | | | <u>32.75,</u> <u>32.92</u> | <u>1.31-1.34</u> | |
| <u>A16, A16', B16, B16'</u> | | <u>34.30</u> | | <u>1.06 ; 1.22</u> | |
| <u>A17, A17', B17, B17'</u> | <u>19.70</u> | | | <u>0.85 - 0.87</u> | Resolved from methyl group signals of A/B 18/18', 19/19' and 20/20' in ¹ H- ¹³ C HSQC. Two sets of doublets resolved in 1D but not assignable to A or B from 2D spectra. |
| <u>A18, A18', B18, B18'</u> <u>A19, A19', B19, B19'</u> <u>A20, A20', B20, B20'</u> | <u>19.85</u> | | | <u>0.83 (app.</u> <u>D, J = 7.7</u> <u>Hz)</u> | Large apparent doublet arising from the 12 methyl groups. |
| <u>Glycerol moiety</u> | | | | | |
| <u>C1</u> | | <u>63.03</u> | | <u>3.58 ; 3.68</u> | ¹ H- ¹³ C HSQC, methylene signal (negative), non-degenerate proton signals. Clear TOCSY correlations from 3.68 ppm |

| | | | | | |
|---------------------------|--------------|--------------|--------------|---|--|
| | | | | | (resolved) to 3.58, 3.51, 3.49 and 3.44 ppm. Weak ^1H - ^{13}C HMBC correlation to C2, correlation to C3 also visible. |
| <u>C2</u> | | | <u>78.31</u> | <u>3.49</u> | |
| <u>C3</u> | | <u>71.07</u> | | <u>3.44 ; 3.51</u> | |
| <u>Butanetriol moiety</u> | | | | | |
| <u>C1'</u> | | <u>61.91</u> | | <u>3.67 (d, $J = 5.0$ Hz)</u> | ^1H - ^{13}C HSQC; single degenerate methylene resonance. ^1H - ^{13}C HMBC; correlations to C2' and C3'. |
| <u>C2'</u> | | | <u>82.38</u> | <u>3.17 (dt, $J = 4.9, 5.3$ Hz)</u> | ^1H - ^{13}C HSQC; methine resonance, C-O chemical shift. ^1H - ^{13}C HMBC; correlations weak due to multiplicity, but could observe correlation to A1' through ether linkage. |
| <u>C3'</u> | | | <u>76.74</u> | <u>3.47</u> | ^1H - ^{13}C HSQC; methine resonance, C-O chemical shift. ^1H - ^{13}C HMBC; correlations to C2' and B1' (through ether linkage). |
| <u>C4'</u> | <u>16.62</u> | | | <u>1.18 (d, $J = 6.7$ Hz but overlapped in 1D)</u> | ^1H - ^{13}C HSQC; Single methyl resonance. ^1H - ^{13}C HMBC; correlations to C2' and C3'. Characteristic coupling to C3' proton observed in ^1H - ^1H COSY spectrum as well as correlations to C2' and C1' protons in the TOCSY spectrum. |

Figures



580 **Figure 1:** Sampling sites in the Black Sea and Mediterranean Sea. The map was generated with GMT software (Wessel et al., 2013).



585 **Figure 2:** Detailed structure of (a) BDGT-0 isolated from *M. luminyensis* and (b) hypothetical structure of PDGT-0 based on Zhu et al. (2014). Carbon numbers in (a) correspond to those given in Table 1, with C4' representing the additional carbon detected in BDGTs.

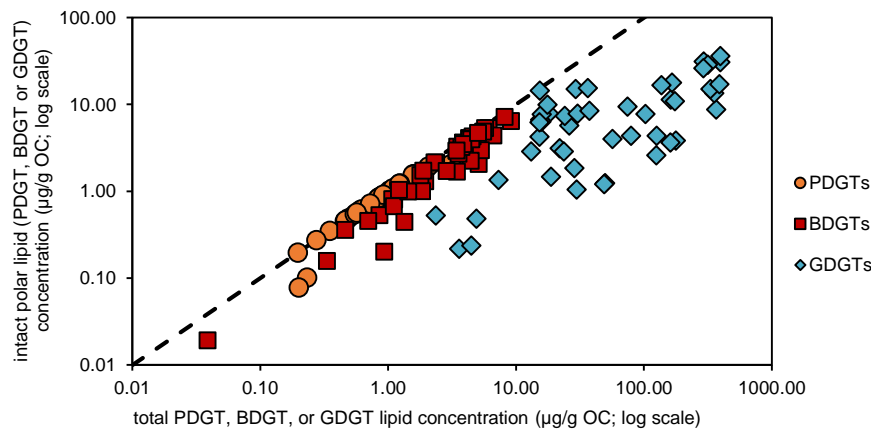


Figure 3: Intact polar lipid concentration against total lipid concentration (log scales) for each archaeal lipid type discussed in this study (PDGTs in orange, BDGTs in red and GDGTs in blue). The dashed line represents the 1:1 line.

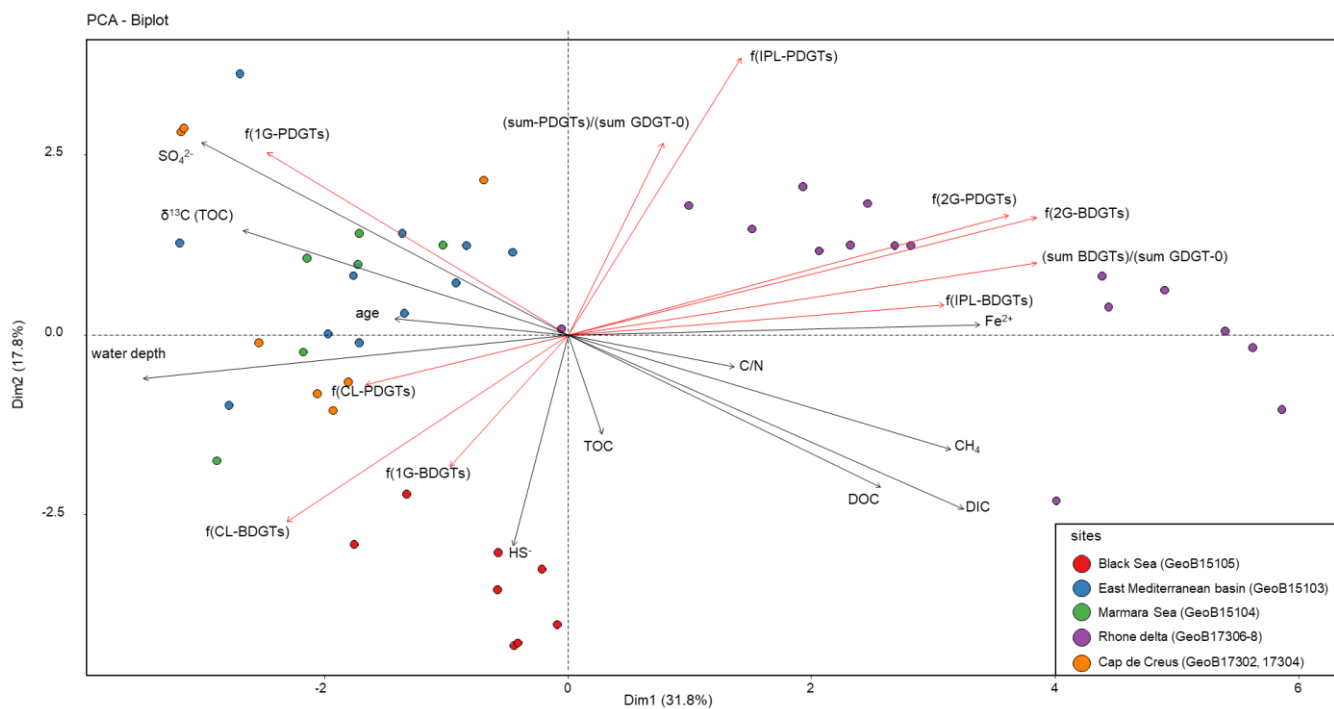


Figure 4: Principal Component Analysis (PCA) biplot showing relationships between major geochemical parameters (grey arrows), indices illustrating BDGT and PDGT distribution (red arrows), and 45 sediment samples (filled circles) from the Mediterranean and Black Seas where BDGTs and PDGTs were detected.

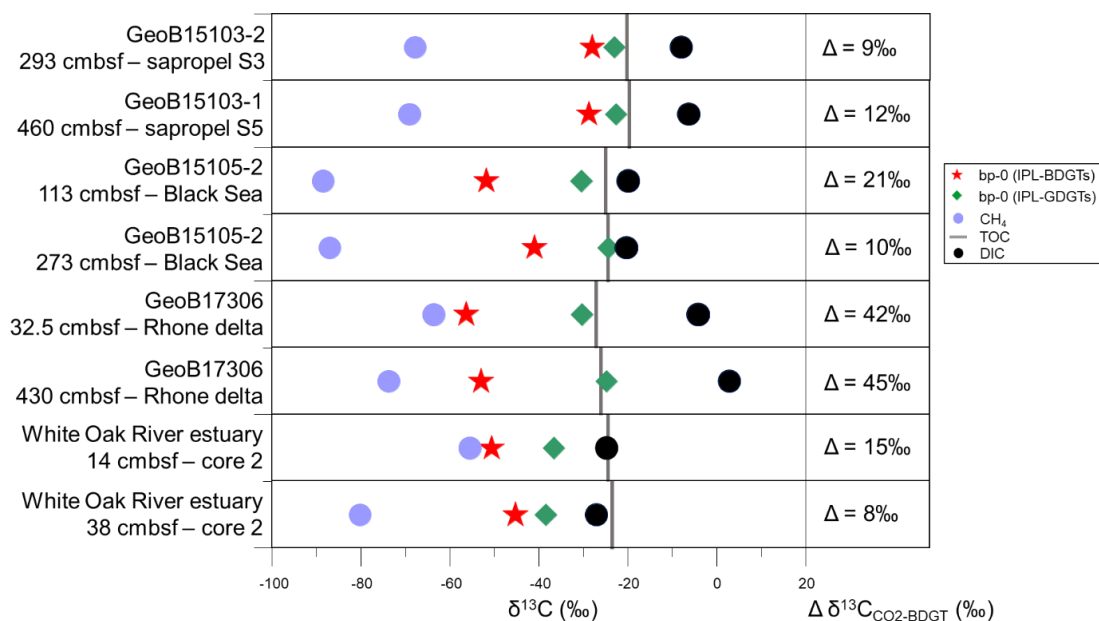


Figure 5: Stable carbon isotopic composition ($\delta^{13}\text{C}$) of bp-0 (IPL-BDGTs) (red stars), bp-0 (IPL-GDGTs) (green diamonds), CH₄ (light blue circles), DIC (black circles), TOC (grey bars) in six selected marine sediment samples from the Mediterranean Sea and Black Sea as well as from the White Oak River Estuary (Meador et al., 2015). Lipid samples were measured in duplicate and are presented as averages; deviations between individual measurements were generally smaller than the symbol size. On the right panel, the difference (Δ) between $\delta^{13}\text{C}_{\text{CO}_2}$ and $\delta^{13}\text{C}_{\text{BDGT}}$ is computed for each sample. $\delta^{13}\text{C}_{\text{CO}_2}$ was ~~calculated~~ derived from $\delta^{13}\text{C}_{\text{DIC}}$ based on an isotope fractionation of -10.7‰ between dissolved CO₂ and DIC, considering in situ temperatures to be below 10°C , according to Mook et al. (1974).